J. Plasma Phys. (2022), *vol*. 88, 905880202
Published by Cambridge University Press
doi:10.1017/S0022377822000022

Effects of intermittency via non-Gaussianity on turbulent transport in magnetized plasmas

D.I. Palade [1],† **and L. Pomârjanschi**[2]

[1]National Institute of Laser, Plasma and Radiation Physics, Atomiștilor Street 409, 077125 Măgurele, Bucharest, Romania

[2]Faculty of Physics, University of Bucharest, Atomiștilor Street 405, 077125 Măgurele, Romania

(Received 15 September 2021; revised 1 January 2022; accepted 4 January 2022)

We analyse how the turbulent transport of $\boldsymbol{E} \times \boldsymbol{B}$ type in magnetically confined plasmas is affected by the intermittent features of turbulence. The latter are modelled via the non-Gaussian distribution $P(\phi)$ of the turbulent electric potential ϕ. Our analysis is performed at an analytical level and confirmed numerically using two statistical approaches. We have found that the diffusion is inhibited linearly by intermittency, mainly via the kurtosis of the distribution $P(\phi)$. The associated susceptibility for this linear process is shown to be dependent on the poloidal velocity V_p and on the correlation time τ_c (or the Kubo number $K_\star$, the ratio between τ_c and the specific time of flight $\tau_{\rm fl}$) with a maximum at $\tau_c \approx \tau_{\rm fl}$ ($K_\star \approx 1$). Intermittency does not affect the scaling of diffusion with the Kubo number.

Keywords: fusion plasma, plasma nonlinear phenomena

1. Introduction

Turbulence plays a major role in the dynamics and confinement of fusion plasmas, both in current and future experimental devices (i.e. ITER Claessens 2020). Low-frequency instabilities evolve and saturate into a turbulent electric field $\boldsymbol{E}$ which, mainly via the $\boldsymbol{E} \times \boldsymbol{B}$ drift ($\boldsymbol{B}$, the magnetic field), tends to transport plasma across magnetic surfaces, toward the walls. Such radial fluxes are particularly dangerous in the scrape-off layer (SOL) region (Krasheninnikov 2001; Lipschultz *et al.* 2007) which absorbs most of the plasma exhaust and transfers it to the divertor. Understanding and controlling this type of transport in tokamak devices has been one of the major challenges for fusion science in the past decades (Bourdelle *et al.* 2007; Angioni *et al.* 2009; Fülöp & Nordman 2009).

Both the edge and the SOL plasma (Zweben *et al.* 2007) are characterized by the presence of intermittent phenomena comparable in magnitude to the amplitude of turbulence. Intermittency (Antar *et al.* 2001*b*) is represented by transient, coherent structures with high density gradients such as blobs (Antar *et al.* 2001*a*; Pereira *et al.* 2019; Cheng *et al.* 2010), Alfvén modes or edge-localized modes (Leonard 2014; Zohm 1996). The emergence of such rare, high-amplitude, fluctuations is captured at a statistical level, through the distribution $P(\phi)$ of electric field values $\phi(\boldsymbol{x}, t)$, which is non-Gaussian. Implicitly, the departure from Gaussianity is characteristic also for field derivatives

† Email address for correspondence: dragos.palade@inflpr.ro

$\partial_t\phi$, $\partial_{ii}\phi$ (Gonçalves *et al.* 2018). The latter are directly related to particle drift and vorticity, and thus to transport.

In the present work we are concerned with understanding and describing how the non-Gaussian features of a turbulent stochastic potential $\phi(\boldsymbol{x}, t)$ affect the transport in the case of a biased, incompressible, two-dimensional velocity field $\boldsymbol{v}(\boldsymbol{x}, t) = \hat{e}_z \times \nabla\phi(\boldsymbol{x}, t) + \boldsymbol{V}_p$. We work in the cartesian coordinate system $\boldsymbol{x} \equiv (x, y, z)$ and $\hat{e}_z$ is the unit vector along the Oz direction. This type of dynamics is relevant not only for the $\boldsymbol{E} \times \boldsymbol{B}$ drift in tokamak plasmas (with $\boldsymbol{B}$ along the Oz direction) in the presence of a poloidal velocity $\boldsymbol{V}_p$, but also for other systems: incompressible fluids, astrophysical plasmas (Zank *et al.* 2011), magnetic field lines wandering (Ghilea *et al.* 2011; Negrea, Petrisor & Shalchi 2017), etc.

Despite the amount of work done within this topic (Corrsin 1951; Kraichnan 1968; Kraichnan & Montgomery 1980; Isichenko 1992; Ottaviani 1992; Reuss & Misguich 1996; Pommois, Veltri & Zimbardo 2001; Vlad *et al.* 1998*a*, 2001), the problem of turbulent transport is, in general, poorly understood due to its complex features. The essence of the problem can be stated as follows: we do not have simple ways to evaluate the diffusion coefficients from the Eulerian properties of the velocity field. Moreover, non-Gaussianity is rarely taken into account, by accident, when simulating realistic flows, thus little it is known about its effects. A solid understanding of such processes might enable possibilities of controlling the turbulent transport in fusion devices and its damaging consequences.

The present theoretical analysis requires *a priori* knowledge of the statistical properties of the potential ϕ: the turbulence spectrum $S(\boldsymbol{k}, \omega)$ and the distribution $P(\phi)$. To acquire such information, one needs to use high-quality gyro-kinetic simulations (Jenko & Dorland 2001; Wang *et al.* 2006) complemented by diagnostic techniques (Casati *et al.* 2009; Gao *et al.* 2015; Gonçalves *et al.* 2018). In tokamak devices, the spectrum shows a fast decay in frequency and along the radial direction with a peaked profile (at some specific wavenumber k_0) along the poloidal direction (Fonck *et al.* 1993; Jenko & Dorland 2002; Casati *et al.* 2009; Holland *et al.* 2009; Shafer *et al.* 2012; Qi *et al.* 2019). One can use the spectrum $S(\boldsymbol{k}, \omega) = \langle|\tilde{\phi}(\boldsymbol{k}, \omega)|^2\rangle$ with $\boldsymbol{k}$ the wavevector and ω the frequency, to derive, as a Fourier transform, under the assumption of homogeneity, the auto-correlation function $\mathcal{E}(\boldsymbol{x}, \boldsymbol{x}'; t, t') = \langle\phi(\boldsymbol{x}, t)\phi(\boldsymbol{x}', t')\rangle \equiv \mathcal{E}(\boldsymbol{x} - \boldsymbol{x}'; t - t')$.

Regarding the probability distribution function (PDF) $P(\phi)$, the experimental evidence (van Milligen *et al.* 2005; Gonçalves *et al.* 2018; Riva *et al.* 2019; Wang *et al.* 2019; Beadle & Ricci 2020) indicates that, in the edge and SOL regions, the potential is approximately Gaussian $P(\phi) \sim \exp(-\phi^2)$ at negative values $\phi < 0$ and has an exponential-like distribution $P(\phi) \sim \exp(-\lambda|\phi|)$ in the positive range $\phi > 0$. This is equivalent with a change both of the skewness and kurtosis of the distribution. Note that the departure from Gaussianity is rather the rule than the exception: all turbulence models (Navier–Stokes, Hasegawa–Mima, Vlasov–Maxwell, etc.) include convective nonlinearities which lead, implicitly, to non-Gaussian solutions (Anderson & Botha 2015; Anderson & Hnat 2017).

The paper is structured as follows. Section 2 is dedicated to a description of the model used to simulate non-Gaussian plasma turbulence. Two methods, the decorrelation trajectory method (DTM), 2.2, and direct numerical simulation (DNS), 2.3, used to investigate the diffusive transport are also briefly presented. Section 3 is devoted to a three step analysis: semi-analytical estimations of the diffusive transport are provided in 3.1, which are further confirmed and refined by a two-level numerical analysis in 3.2, which is finally explained from a microscopic point of view in 3.3. Finally, § 4 is dedicated to conclusions and perspectives.

https://doi.org/10.1017/S0022377822000022 Published online by Cambridge University Press

2. Theory

We describe the motion of ions in a magnetically confined plasma using a simple geometric set-up: the strong magnetic field is considered constant $\boldsymbol{B} = B_0\hat{e}_z$ while the ions are subject to a drift-type motion in the perpendicular plane $\boldsymbol{x} \equiv (x, y)$ in the presence of an effective poloidal velocity (originating from magnetic drifts or plasma rotation) $\boldsymbol{V}_p \equiv V_p\hat{e}_y$

$$\frac{\mathrm{d}\boldsymbol{x}(t)}{\mathrm{d}t} = \hat{e}_z \times \nabla\phi(\boldsymbol{x}(t), t) + V_p\hat{e}_y. \tag{2.1}$$

The statistical description of transport in this context is as follows (Palade 2021; Vlad, Palade & Spineanu 2021): an ensemble of stochastic fields $\{\phi(\boldsymbol{x}, t)\}$ with known Eulerian properties is considered to drive an associated ensemble of trajectories via equation (2.1). The diffusion coefficient is computed as the Lagrangian correlation $D(t) = 1/2d_t\langle \boldsymbol{x}^2(t)\rangle \equiv \langle \boldsymbol{v}(0)\boldsymbol{x}(t)\rangle$ with the initial conditions $\boldsymbol{x}(0) = 0$. Using the characteristic correlation length λ_c, correlation time τ_c and velocity amplitude $V = \Phi/\lambda_c$, $\Phi = \sqrt{\langle\phi^2(\boldsymbol{0}, 0)\rangle}$, one can define the Kubo number (Vlad *et al.* 1998*a*) $K_\star$

$$K_\star = \frac{\tau_c}{\tau_{\mathrm{fl}}} = \frac{V\tau_c}{\lambda_c} = \frac{\Phi\tau_c}{\lambda_c^2}, \tag{2.2}$$

as a measure of the correlation time relative to the specific time of flight $\tau_{\mathrm{fl}} = \lambda_c/V$. Another interpretation of $K_\star$ is that of turbulence strength. Consequently, one can distinguish two regimes of transport: the quasilinear (weak/high-frequency turbulence, $K_\star \ll 1$) and the strong/low-frequency ($K_\star \gg 1$) regimes. The quasilinear asymptotic diffusion coefficient can be exactly evaluated as $D^\infty \sim K_\star^2\lambda_c^2/\tau_c$ while in the strong limit the transport is anomalous $D^\infty \sim K_\star^{1-\gamma}$ with $\gamma \in (0, 1)$. Although still under debate, it has been proposed (Isichenko 1992) and confirmed within some degree of numerical error (Ottaviani 1992; Reuss & Misguich 1996; Hauff & Jenko 2006) that the anomalous exponent is roughly $\gamma \approx 3/10$.

2.1. *Turbulence description*

The statistical approach to turbulent transport requires the modelling of the potential ϕ as a non-Gaussian, zero-averaged, homogeneous random field. In order to do that, we assume (as a technical commodity Vio, Andreani & Wamsteker 2001; Liu *et al.* 2019; Palade & Vlad 2021) that the non-Gaussian field $\phi(\boldsymbol{x}, t)$ can be related to another, fictitious, Gaussian field $\varphi(\boldsymbol{x}, t)$ with known correlation function $\mathcal{E}(\boldsymbol{x} - \boldsymbol{x}', t - t') = \langle\varphi(\boldsymbol{x}, t)\varphi(\boldsymbol{x}', t')\rangle$ via a nonlinear transformation $\phi(\boldsymbol{x}, t) = f(\varphi(\boldsymbol{x}, t))$. The function f must be chosen such that both fields are zero averaged $\langle\phi(\boldsymbol{x}, t)\rangle = \langle\varphi(\boldsymbol{x}, t)\rangle = 0$ and have the same amplitude of fluctuations $\langle\phi^2(\boldsymbol{x}, t)\rangle = \langle\varphi^2(\boldsymbol{x}, t)\rangle = \mathcal{E}(\boldsymbol{0}, 0) = V_0$.

It can be easily proven that a local nonlinear transformation preserves the homogeneity property. This means that the field $\phi(\boldsymbol{x}, t)$ is also homogeneous, i.e. its correlation function is only distance dependent $\langle\phi(\boldsymbol{x}, t)\phi(\boldsymbol{x}', t')\rangle = \langle f(\varphi(\boldsymbol{x}, t))f(\varphi(\boldsymbol{x}', t'))\rangle = \mathcal{E}'(\boldsymbol{x} - \boldsymbol{x}', t - t')$.

Straightforwardly, we can generically compute the correlation of the derivatives as well as the skewness s and the excess kurtosis $\delta\kappa$ of the non-Gaussian field ϕ

$$\langle\partial_i\phi(\boldsymbol{x}, t)\partial_j\phi(\boldsymbol{x}', t')\rangle = \langle f'[\varphi(\boldsymbol{x}, t)]\, f'\left[\varphi(\boldsymbol{x}', t')\right]\partial_i\varphi(\boldsymbol{x}, t)\partial_j\varphi(\boldsymbol{x}', t')\rangle, \tag{2.3}$$

$$s = \frac{\langle\phi^3\rangle}{\langle\phi^2\rangle^{3/2}} = \frac{\langle f^3[\varphi]\rangle}{\langle f^2[\varphi]\rangle^{3/2}}, \tag{2.4}$$

https://doi.org/10.1017/S0022377822000022 Published online by Cambridge University Press

$$\delta\kappa = \frac{\langle\phi^4\rangle}{\langle\phi^2\rangle^2} - 3 = \frac{\langle f^4[\varphi]\rangle}{\langle f^2[\varphi]\rangle^2} - 3. \tag{2.5}$$

Experimental measurements in the SOL of various tokamak devices (Filippas *et al.* 1995; Antar *et al.* 2001*a*,*b*; van Milligen *et al.* 2005; Casati *et al.* 2009; Riva *et al.* 2019) have shown PDFs of electrostatic fluctuations which exhibit longer tails as well as skewness, especially in the positive part of the distribution. For these reasons, we choose a particularly simple nonlinear transformation to construct the non-Gaussian fields: $f(\varphi) \sim \varphi + \alpha\varphi^2 + \beta\varphi^3 - \alpha V_0$

$$\phi = \frac{\varphi + \alpha\varphi^2 + \beta\varphi^3 - \alpha V_0}{\sqrt{1 + 2\alpha^2 V_0 + 3\beta V_0(2 + 5\beta V_0)}}, \tag{2.6}$$

$$\partial_i\phi = \frac{1 + 2\alpha\varphi + 3\beta\varphi^2}{\sqrt{1 + 2\alpha^2 V_0 + 3\beta V_0(2 + 5\beta V_0)}}\partial_i\varphi, \tag{2.7}$$

$$s \approx 6\alpha V_0^{1/2}(1 + 3V_0\beta), \tag{2.8}$$

$$\delta\kappa \approx 24\beta V_0 + 144 V_0^2\beta^2 + 48 V_0\alpha^2, \tag{2.9}$$

$$\mathcal{E}' = \frac{\mathcal{E}\left(2\alpha^2\mathcal{E} + 6\beta^2\mathcal{E}^2 + (3\beta V_0 + 1)^2\right)}{1 + 2\alpha^2 V_0 + 3\beta V_0(5\beta V_0 + 2)}. \tag{2.10}$$

Note that, up to first order, the skewness is controlled by the α parameter and the kurtosis by β. Also, the correlation is virtually unchanged due to its second-order parametric dependence $\mathcal{E}' \approx \mathcal{E} + 2\alpha^2\mathcal{E}(\mathcal{E} - V_0) + 6\beta^2\mathcal{E}(\mathcal{E}^2 - V_0^2)$. This enables us to approximate $\mathcal{E}' \approx \mathcal{E}$ since $\alpha, \beta \sim 10^{-2,-1}$ for a good agreement with experimental distributions (Filippas *et al.* 1995; Riva *et al.* 2019).

We note that the presence of a poloidal velocity field V_p implies that the turbulent field ϕ moves with this velocity, which should modify the turbulence statistics. However, since we consider a homogeneous turbulence and the experimental measurements of field statistics are usually performed in the laboratory system, such modifications are not present.

Our model of intermittency (2.6) captures the stochastic features of turbulence (ϕ being a random field) and also the departure from a Gaussian distribution (through the $f(\cdot)$ transformation). Yet, we acknowledge that true intermittency exhibits other features such as scale symmetry breaking and deviation from homogeneity. Such elements are beyond the scope of the present work.

2.2. *Decorrelation trajectory method*

The DTM has been used in the past decades to investigate various types of turbulent transport in tokamak plasmas (Vlad *et al.* 1998*a*, 2004; Vlad & Spineanu 2016; Croitoru *et al.* 2017) as well as in some astrophysical systems (Negrea 2019). The method is semi-analytical, since it describes the transport via a set of deterministic objects called decorrelation trajectories (DTs) (Vlad *et al.* 1998*a*) which are used to compute the diffusion (2.12)

$$\frac{\mathrm{d}\boldsymbol{X}^S(t)}{\mathrm{d}t} = \boldsymbol{V}^S(\boldsymbol{X}^S(t), t) = \hat{e}_z \times \nabla\Phi^S(\boldsymbol{X}^S(t), t) + \boldsymbol{V}_p, \tag{2.11}$$

$$D_{xx}(t) = \langle v_x(0)x(t)\rangle \approx \int \mathrm{d}S\, P(S) V_x^S(\mathbf{0}, 0) X^S(t). \tag{2.12}$$

https://doi.org/10.1017/S0022377822000022 Published online by Cambridge University Press

The main assumption of DTM is that trajectories with similar initial conditions should remain similar at all times. If this is true, one can replace the ensemble of real stochastic potentials $\{\phi(\boldsymbol{x}, t)\}$ with a set of deterministic conditional potentials $\{\Phi^S(\boldsymbol{x}, t)\}$ which are defined as conditional averages over real potentials in sub-ensembles (S), i.e. $\Phi^S(\boldsymbol{x}, t) = \langle\phi(\boldsymbol{x}, t)\rangle^S$. The DTs $\boldsymbol{X}^S(t)$ are solutions for the equation (2.11).

For our non-Gaussian case, we define the sub-ensembles via the initial values (at $\boldsymbol{x} = 0$ and $t = 0$) of the auxiliary field φ as

$$S = \{\phi(\boldsymbol{x}, t) = f\,(\varphi(\boldsymbol{x}, t))\,|\partial_i\varphi(\boldsymbol{0}, 0) = \varphi_i^S;\, i \in \{0, x, y\}\} \tag{2.13}$$

where each S has a probabilistic weight $P(S) = \prod_{i\in\{0,x,y\}} \exp(-(\varphi_i^S)^2/V_{ii}/2)$ with $V_{ii} = \langle[\partial_i\varphi(0)]^2\rangle = -\partial_{ii}\mathcal{E}(0, 0)$. From a straightforward calculus of $\Phi^S = \langle\phi\rangle^S = \langle f(\varphi)\rangle^S$ we complete the DTM model

$$\Phi^S = \frac{\Psi^S(1 + 3\beta\sigma) + \alpha(-1 + \sigma + (\Psi^S)^2) + \beta(\Psi^S)^3}{\sqrt{1 + 2\alpha^2 + 6\beta + 15\beta^2}}, \tag{2.14}$$

$$\Psi^S = \varphi_0^S\frac{\mathcal{E}(\boldsymbol{x}, t)}{V_0} + \varphi_x^S\frac{\partial_x\mathcal{E}_x(\boldsymbol{x}, t)}{V_{xx}} + \varphi_y^S\frac{\partial_y\mathcal{E}_y(\boldsymbol{x}, t)}{V_{yy}}, \tag{2.15}$$

$$\sigma = V_0 - \frac{\mathcal{E}^2}{V_0} - \frac{(\partial_x\mathcal{E})^2}{V_{xx}} - \frac{(\partial_y\mathcal{E})^2}{V_{yy}}. \tag{2.16}$$

The function σ is, in fact, a measure of field fluctuations within a sub-ensemble S which turns out to be independent of S: $\sigma(\boldsymbol{x}, t) = \langle\delta\varphi^2(\boldsymbol{x}, t)\rangle^S$. Note that, in the Gaussian limit $\alpha = \beta = 0$, the model simplifies to $\Phi^S \to \Psi^S$, as has been used in previous studies (Vlad *et al.* 1998*a*; Vlad & Spineanu 2016; Croitoru *et al.* 2017; Negrea 2019). The DTM method is equivalent to neglecting trajectory fluctuations (Vlad *et al.* 1998*b*) within a sub-ensemble. For more details on the method see Vlad *et al.* (1998*a*, 2001, 2004) and Croitoru *et al.* (2017).

2.3. *DNS method*

The purpose of DNS is to investigate turbulent transport as it is, without resorting to any approximations, closures or supplementary models.

In our case, this is achieved by constructing a statistical ensemble of Gaussian random fields (GRFs) $\varphi(\boldsymbol{x}, t)$ with the correct correlation function which will be used to derive the ensemble of non-Gaussian fields ϕ via the prescribed transformation $\phi = f(\varphi)$. For each realization, (2.1) is solved and a trajectory is obtained. The transport coefficients, diffusion and average velocity, are computed as simple statistical averages over the ensemble. DNS tries to mimic the whole (real) statistical problem resorting to numerical tools (Palade 2021; Palade & Vlad 2021; Vlad *et al.* 2021).

We underline that the turbulent character of the potential is captured both by the chaotic nature of the random fields and by the statistical approach, which considers an ensemble of such stochastic objects.

The main source of errors in DNS is an insufficient numerical representation of the ensemble. In practice, we use a spectral representation of GRFs as discussed in Palade & Vlad (2021) with improved Eulerian and Lagrangian convergences

$$\varphi(\boldsymbol{x}) = \sum_j^{N_c} S^{1/2}(\boldsymbol{k}_j)\sin\left(\boldsymbol{k}_j\boldsymbol{x} + \frac{\pi}{4}\zeta_j\right), \tag{2.17}$$

https://doi.org/10.1017/S0022377822000022 Published online by Cambridge University Press

where $\boldsymbol{k}_j$ are randomly distributed within the compact support of the spectrum $S(\boldsymbol{k})$ and $\zeta_j = \pm 1$ is randomly chosen. In practice, we use $N_c \sim 10^d$ as this was found to ensure both the Gaussianity of the field as well as the details of the correlation function. Good statistical convergence is found, both at the Eulerian and Lagrangian levels, to be satisfied by ensembles with dimension $M \sim 10^5$.

This is the standard approach of DNS to transport. It is suitable for GRFs since the field φ is naturally Gaussian via the central limit theorem. In order to tackle the problem of non-Gaussian ϕ, we compute as such (2.17) the fields φ and solve the following equation of motion:

$$\frac{\mathrm{d}\boldsymbol{x}(t)}{\mathrm{d}t} = f'(\varphi(\boldsymbol{x}(t), t))\hat{e}_z \times \nabla\varphi(\boldsymbol{x}(t), t) + \boldsymbol{V}_p. \tag{2.18}$$

Note that the above equation (2.18) is equivalent to (2.1) given the fact that $\phi = f(\varphi)$. The rest of the method remains unchanged. For more details see Palade, Vlad & Spineanu (2021), Hauff & Jenko (2006), Palade & Vlad (2021), Vlad *et al.* (2021) and Palade (2021).

3. Results

In order to capture the basic physical processes related to non-Gaussianity, we use two simple model correlation functions $\mathcal{E}_1$ and $\mathcal{E}_2$ for the φ field

$$\mathcal{E}_1(x, y, t) = \exp\left(-\frac{x^2}{2\lambda_x^2} - \frac{y^2}{2\lambda_y^2} - \frac{t}{\tau_c}\right) \tag{3.1}$$

$$\mathcal{E}_2(x, y, t) = \left(1 + \frac{x^2}{\lambda_x^2} + \frac{y^2}{\lambda_y^2}\right)^{-1} \mathrm{e}^{-t/\tau_c}, \tag{3.2}$$

with $\lambda_x = \lambda_y = 1$ and $\tau_c = 10$. Thus, $V_0 = 1$. These choices are in agreement with the gross features of turbulence spectra from incompressible plasmas and fluids (Levinson *et al.* 1984; Boldyrev 2005; Casati *et al.* 2009; Gao *et al.* 2015).

In figure 1(*a*,*b*) we show how the proposed transformation $f(\varphi) \sim \varphi + \alpha\varphi^2 + \beta\varphi^3 - \alpha$ distorts the Gaussian distribution both for the potential and its derivatives. Note how, through appropriate combinations of α and β (the brown line), the resulting PDF is closer to Gaussianity in the negative domain $\phi < 0$ and similar to an exponential distribution in the positive part $\phi > 0$ (as observed in measurements). Also, due to the relation between $\partial_i\phi$ and φ, the distribution of derivatives $P(\partial_i\phi)$ is free of any skewness.

In figure 2(*a*,*b*) we plot the change in correlation $\delta\mathcal{E} = \mathcal{E}' - \mathcal{E}$ under the effects of non-Gaussianity for the first model, $\mathcal{E}_1$. The results are in agreement with the analytical estimation (2.6) in that the departure is $\delta\mathcal{E} \sim \mathcal{O}(\alpha^2, \beta^2) \sim 1\,\%\mathcal{E}$ and virtually negligible, especially in the strongly correlated area $|\boldsymbol{x}| \sim 0$. For $\mathcal{E}_2$ the profiles are extremely similar.

3.1. *Analytical estimations*

Our first level of analysis is the analytical one. We intend to estimate the change of the diffusion coefficient induced by non-Gaussian features of turbulence. In order to do that, we start by considering a simplified case of frozen turbulence, when the potential is time independent $\varphi(\boldsymbol{x}, t) \equiv \varphi(\boldsymbol{x})$. This case can be obtained setting $\tau_c \to \infty$. Due to the Hamiltonian structure of the equations (2.1), the trajectories are closed and both the fictitious and the real potentials are conserved $\varphi(\boldsymbol{x}(t)) = \varphi(\boldsymbol{x}(0)) = \varphi(\boldsymbol{0}) \implies \phi(\boldsymbol{x}(t)) =$

https://doi.org/10.1017/S0022377822000022 Published online by Cambridge University Press

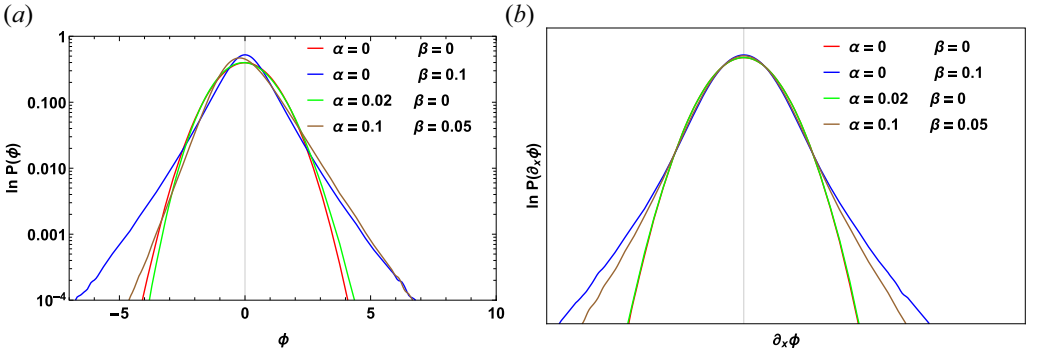

FIGURE 1. PDF of potential values (*a*) and potential derivatives (*b*) generated randomly in accordance with the nonlinear transformation from (2.6).

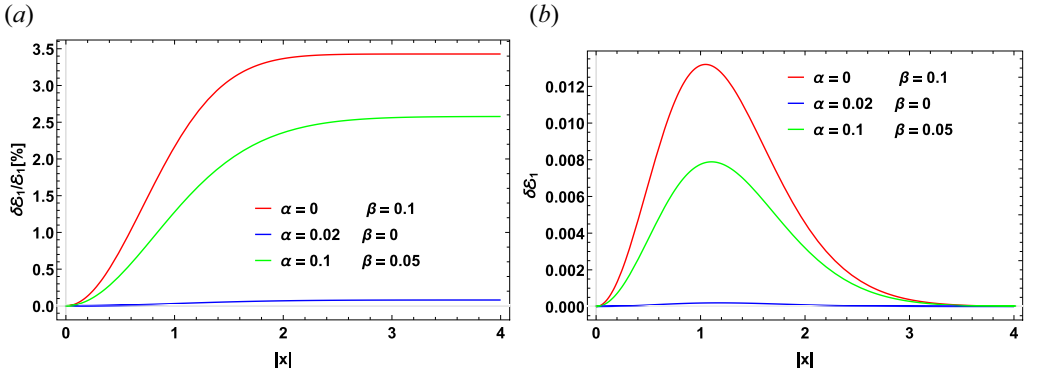

FIGURE 2. Relative changes $\delta\mathcal{E}_1 = \mathcal{E}_1' - \mathcal{E}_1$ of the correlation function in the spatial domain at different small α, β values.

$\phi(\boldsymbol{x}(0)) = \phi(\boldsymbol{0})$. For further purposes, let us denote the following function:

$$A[\varphi] = \frac{1 + 2\alpha\varphi + 3\beta\varphi^2}{\sqrt{1 + 2\alpha^2 + 3\beta(2 + 5\beta)}}. \tag{3.3}$$

With this notation, it turns out that the equations of motion in the Gaussian and non-Gaussian (0 index) cases become

$$\frac{\mathrm{d}\boldsymbol{x}_0(t)}{\mathrm{d}t} = \hat{e}_z \times \nabla\varphi(\boldsymbol{x}_0(t)), \tag{3.4}$$

$$\frac{\mathrm{d}\boldsymbol{x}(t)}{\mathrm{d}t} = A[\varphi(0)]\hat{e}_z \times \nabla\varphi(\boldsymbol{x}(t)). \tag{3.5}$$

It can be easily shown, via a variable transformation, that $\boldsymbol{x}(t) = \boldsymbol{x}_0(A[\varphi(\boldsymbol{0})]t)$. This exact relation allows us to relate the running diffusion coefficients between these two cases, non-Gaussian $D(t)$ and the Gaussian limit $D_0(t)$. In order to do that, let us denote the 'conditional diffusion' for trajectories starting at equal potential values as

$$d_0(t; \varphi(\boldsymbol{0})) = \frac{1}{2}\frac{\mathrm{d}}{\mathrm{d}t}\langle \boldsymbol{x}_0^2(t)\rangle_{\varphi(\boldsymbol{0})} \tag{3.6}$$

https://doi.org/10.1017/S0022377822000022 Published online by Cambridge University Press

for which it holds true that $d(t;\varphi(\mathbf{0})) = A[\varphi(\mathbf{0})]d_0(A[\varphi(\mathbf{0})]t;\varphi(\mathbf{0}))$. Finally, we write

$$D_0(t) = \int \mathrm{d}\varphi(0) P[\varphi(\mathbf{0})] d_0(t;\varphi(\mathbf{0})), \tag{3.7}$$

$$D(t) = \int \mathrm{d}\varphi(0) P[\varphi(\mathbf{0})] d_0(A[\varphi(\mathbf{0})]t;\varphi(\mathbf{0}))A[\varphi(\mathbf{0})]. \tag{3.8}$$

Without any proof, we assume that some sort of generalized mean value theorem is valid and these two integrals can be related through an effective potential

$$D(t) = A[\varphi_{\mathrm{eff}}(t)] D_0(A[\varphi_{\mathrm{eff}}(t)]t). \tag{3.9}$$

On the other hand, the anomalous feature of transport is reflected in the asymptotic behaviour of running Lagrangian averages $L(t)$ which algebraically decay $L_0(t) \sim t^{-\gamma}$ (Isichenko 1992; Ottaviani 1992; Reuss & Misguich 1996; Reuss, Vlad & Misguich 1998; Vlad *et al.* 1998*a*, 2004). At small times $t \ll \tau_{\mathrm{fl}}$ the dependence of $L(t)$ can usually be analytically computed. The presence of a decorrelation mechanism (finite τ_c in our case) tends to saturate asymptotically all Lagrangian quantities at values which can be estimated (Vlad *et al.* 1998*a*, 2004) as $\lim_{t\to\infty} L(t) = L^\infty \approx L(\tau_c)$. We assume this to be true both for diffusion $D(t)$ and $\varphi_{\mathrm{eff}}(t)$.

Combining all these behaviours, the algebraic decay $D(t) \sim t^{-\gamma}$, $\varphi_{\mathrm{eff}}(t) \sim t^{-\zeta}$, the approximate saturation at the decorrelation time $D^\infty \approx D(\tau_c)$, $\varphi^\infty_{\mathrm{eff}} \approx \varphi_{\mathrm{eff}}(\tau_c)$ and the assumed relation between Gaussian and non-Gaussian diffusion (3.9), one can show that

$$\begin{cases} D^\infty/D_0^\infty = A[\varphi_{\mathrm{eff}}(\tau_c;\alpha,\beta)]^2 \approx 1 + 2\alpha^2 + 12\beta^2, & K_\star \ll 1 \\ D^\infty/D_0^\infty = A[\varphi_{\mathrm{eff}}(\tau_c;\alpha,\beta)]^{1-\gamma} \approx 1 + 3\beta(-1+\gamma), & K_\star \gg 1. \end{cases} \tag{3.10}$$

These estimations suggest that α has only a quadratic effect on the diffusion coefficient. This aspect can be understood from another perspective, analysing how the Lagrangian correlation of velocities $L_v(t) = \langle v_x(0)v_x(t)\rangle$ (the time derivative of $D(t)$) varies with α up to the first order

$$\frac{\partial}{\partial\alpha} L_v(t) = \frac{\partial}{\partial\alpha}\langle v_x(\mathbf{0},0)v_x(\boldsymbol{x}(t),t)\rangle \propto \langle\varphi(0)\partial_y\varphi(0)\partial_y\varphi(t)\rangle + \langle\varphi(t)\partial_y\varphi(0)\partial_y\varphi(t)\rangle \approx 0. \tag{3.11}$$

Note that $\varphi(0)$ and $\partial_i\varphi(0)$ are uncorrelated Gaussian quantities. Moreover, Lumley's theorem (Monin & Yaglom 1973) assures us that the space derivatives $\partial_i\varphi(t)$ remain Gaussian quantities at all times. Only the distribution of Lagrangian potentials $\varphi(t)$ might depart from Gaussianity in the case of finite τ_c, but only slightly. Thus, the derivative $\partial_\alpha L_v(t)$ is roughly made up of averages of products of three Gaussian quantities and, therefore, is zero. This means that $L_v(t)$ is roughly independent of α up to first order. The same goes for the diffusion.

Following the above reasoning and estimations (3.10), we expect that the non-Gaussian diffusion will vary roughly as $\mathcal{O}(\beta)$, $\mathcal{O}(\alpha^2)$. For this reason, we define a response function (susceptibility χ) to quantify the possible linear dependency between diffusion variation and turbulence excess kurtosis (as a measurable quantity)

$$\chi = \lim_{\delta\kappa\to 0} \frac{1}{\delta\kappa}\left(1 - \frac{D^\infty(\delta\kappa)}{D^\infty(0)}\right). \tag{3.12}$$

https://doi.org/10.1017/S0022377822000022 Published online by Cambridge University Press

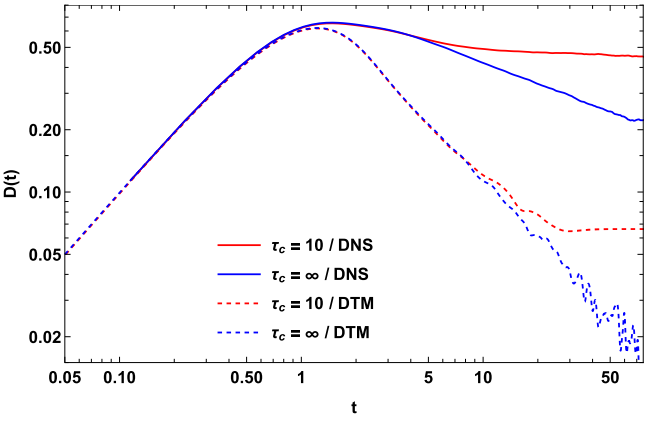

FIGURE 3. Running diffusion coefficient $D(t)$ obtained for the correlation $\mathcal{E}_1$, $V_p = 0$ in the case $\tau_c \to \infty$ (blue) and $\tau_c = 10$ (red) with the use of DNS (full line) and DTM (dashed line).

3.2. *Numerical results*

We intend to test further if the analytical estimations found above bear any meaning in real situations. For that, we use the statistical methods described previously: DNS and DTM. We underline that DNS is an exact-in-principle method which is hindered in practice only by the numerical resolution, thus, it requires a large amount of CPU resources. DTM is an approximation which provides only qualitative results and it is easy to implement numerically. The purpose of DTM in this work is to serve as a supplementary test for the results of DNS which might be plagued with a small, but uncertain, degree of numerical inaccuracy.

We perform numerical simulations of the running diffusion coefficients $D(t)$ for the incompressible motion (2.1) where the potential $\phi(\boldsymbol{x}, t)$ is described via a fictitious field $\varphi(\boldsymbol{x}, t)$ (2.6) with known Eulerian correlation (3.1). The numerical method for trajectory propagation both in (2.18) (DNS) and (2.11) (DTM) is a fourth-order Runge–Kutta method with a fixed time step $\Delta t \sim 10^{-1} \min(\tau_c, \lambda_c^2)$. The simulation time is $t_{\max} \sim 5\tau_c$. The number of trajectories simulated with DNS is routinely $N_p \sim 10^5$ while the number of sub-ensembles used in DTM $N_s \sim 10^5$. These resolutions are chosen for numerical accuracy and statistical precision. Using dedicated programming procedures, typical simulations on personal computers require in terms of CPU time $t_{\mathrm{CPU}}^{\mathrm{DTM}} \sim 1$ min and $t_{\mathrm{CPU}}^{\mathrm{DNS}} \sim 10$ min.

Beyond diving into the matter of non-Gaussianity, let us have a look at a typical running diffusion coefficient $D(t)$ obtained in the case $\alpha = \beta = 0$. The results of both methods are shown in figure 3 at $\tau_c = 10$ and $\tau_c \to \infty$. In the case of frozen turbulence one can see the algebraic decay of diffusion $D(t) \sim t^{-\gamma}$. The effect of finite τ_c is the saturation of diffusion to a constant value $D^\infty = D(t \to \infty)$. Note that DTM reproduces the qualitative behaviour of trapping and decorrelation at all times. Yet, the results are quantitatively different in the asymptotic region $t \gg \tau_{\mathrm{fl}}$. This is a due to the overestimation of trapping in the DTM approximation. Consequently, DTM overestimates the γ exponent too and we expect it will overestimate the effect of intermittency in the strong/low-frequency turbulence regime.

We investigate further the dependence of the diffusion on α and find that both methods, DTM and DNS, predict a negligible variation (figure 4). The results are in line with our analytical estimation that α affects the transport only at second order. A very weak linear dependence supplemented by a weak quadratic one can be observed.

https://doi.org/10.1017/S0022377822000022 Published online by Cambridge University Press

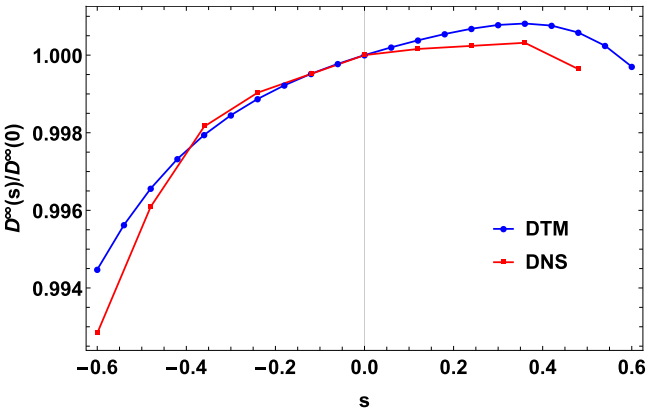

FIGURE 4. Asymptotic values of diffusion at $\beta = 0$, $\tau_c = 10$, $V_p = 0$ vs the skewness s obtained with the use of DTM (blue line) and DNS (red line).

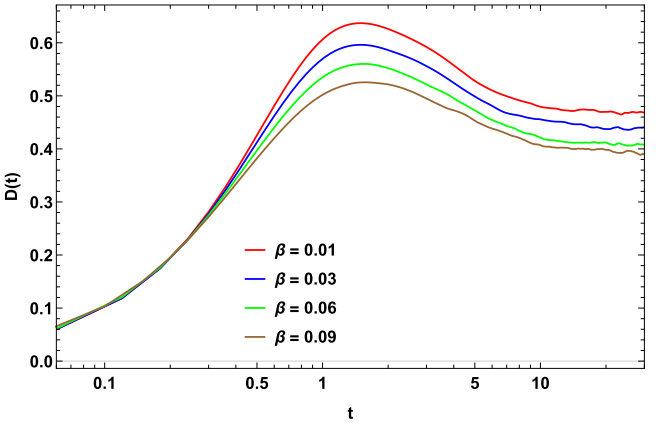

FIGURE 5. Running diffusion profiles $D(t)$ obtained with DNS for the correlation $\mathcal{E}_1$ with $\tau_c = 10$ and $V_p = 0$ at different β values and $\alpha = 0$.

Given this fact, let us set $\alpha = 0$ and look further at how β affects the diffusion. The mechanism can be seen at work in figure 5, where several running diffusion profiles $D(t)$ are shown for different β values. As expected, the effect is visible only at larger times, at least at the order of τ_{fl}, and it results in a decrease of the diffusion coefficient. This behaviour can be quantified further by inspecting the variation of the asymptotic diffusion D^{∞} with β.

We plot in figure 6 asymptotic diffusion coefficients computed for different values of β with DNS (blue) for the correlation function $\mathcal{E}_1$ and with DTM (red) for $\mathcal{E}_2$. Our expectation that the β parameter drives a linear change in the diffusion is confirmed. Also, it must be emphasized how close the results of DTM to those of DNS are, given the fact that they use two distinct correlations.

Going further into understanding the effects of intermittency, we plot in figure 7 profiles of asymptotic diffusion coefficients vs the Kubo number at different values of the β parameter. As expected from the results of figure 6 the effect of β is to inhibit the overall values of diffusion. However, something supplementary must be underlined: in the high $K_\star$ region, that of trajectory trapping, the profiles are approximately parallel to each other

https://doi.org/10.1017/S0022377822000022 Published online by Cambridge University Press

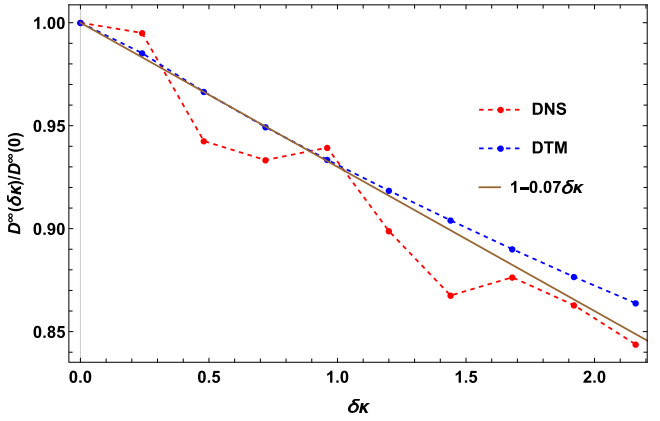

FIGURE 6. The relative asymptotic diffusion dependence on the excess kurtosis obtained with DTM for $\mathcal{E}_2$ (blue line) and with DNS for $\mathcal{E}_1$ (red line).

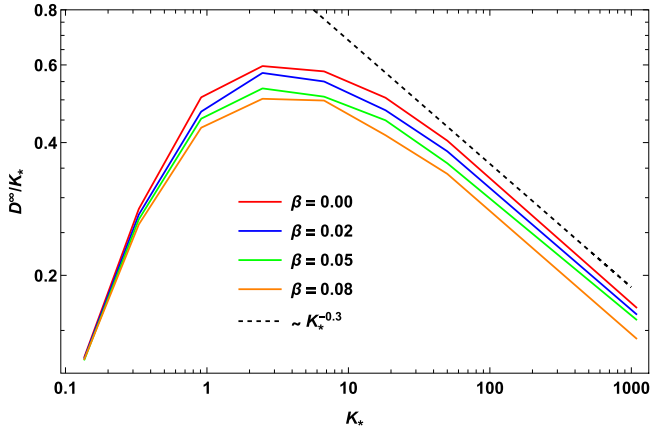

FIGURE 7. Asymptotic diffusion coefficient vs the Kubo number at different β values. The results are obtained with DNS for $\mathcal{E}_1$ and $V_p = 0$.

and to the $\sim K_\star^{-0.3}$ line. This tells us that the Kubo number scaling is universal $\gamma = 0.3$ and it is unaffected by non-Gaussianity.

After confirming the linear behaviour in β, we look into the dependence of the susceptibility χ on the Kubo number $K_\star$. We have performed extensive numerical simulations both with DTM and DNS varying both the Kubo number (through τ_c) and the β parameter. Final results are shown in figure 8, where we plot $\chi(K_\star)$ obtained with DNS at several distinct V_p values. As one can see, at small correlation times, this quantity is null. It increases only quadratically with $K_\star$, until around τ_c of the order of the time of flight and saturates for $V_d = 0$. An interesting effect of the average velocity can be seen in figure 8, which consists in the strong attenuation of the effect of the kurtosis. The susceptibility has a strong algebraic decay in these conditions.

In figure 9 we show the profile of χ obtained with DTM in the case of $V_p = 0$. The method is able to confirm what was found with DNS: the susceptibility grows to a maximum around the time of flight and decays at larger values of $K_\star$. As expected, since DTM overestimates the trapping, it also overestimates the decay of χ.

https://doi.org/10.1017/S0022377822000022 Published online by Cambridge University Press

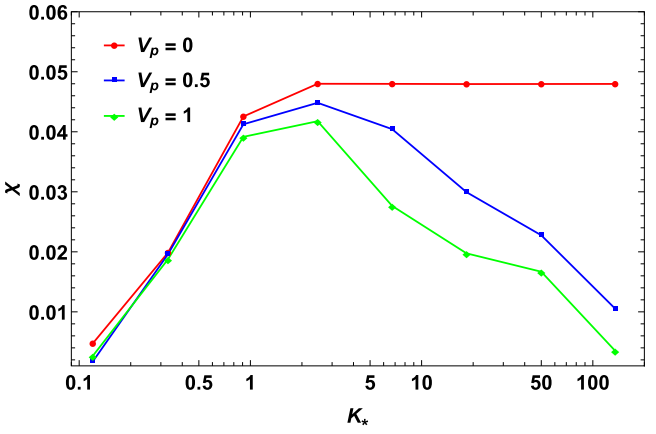

FIGURE 8. Susceptibility χ as a function of Kubo number $K_\star$ obtained with DNS for $\mathcal{E}_1$ at distinct V_p values.

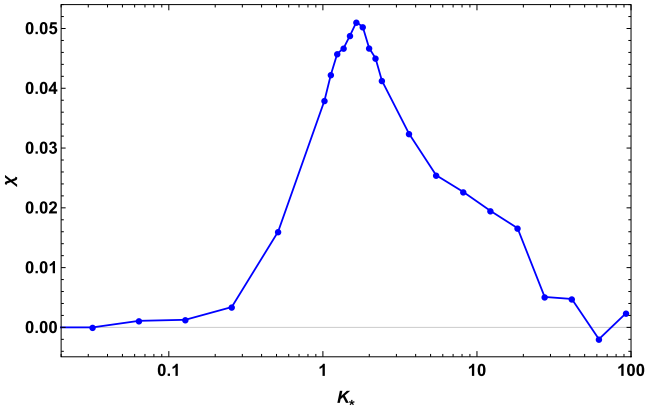

FIGURE 9. Susceptibility χ as a function of Kubo number $K_\star$ obtained with DTM for $\mathcal{E}_2$ at $V_p = 0$.

We underline that high Kubo number regimes $K_\star \gg 1$ are less relevant for a realistic tokamak plasma. Yet, we have considered in our simulations a wide parametric region $K_\star \in (0, 100)$ in order to offer a complete, quantitative, representation of the effects found.

3.3. *Microscopic analysis*

The effect of non-Gaussianity on transport can be understood from a microscopic perspective, following how individual trajectories change, or how their statistics is modified.

One can start the analysis from the limiting case of frozen turbulence $\tau_c \to \infty$. While the trajectories remain unchanged (see § 3.1) the velocity is changed by a factor $A[\varphi(\mathbf{0})]$. The consequence is that the diffusion across that particular equipotential line becomes $d(t; \varphi(\mathbf{0})) = A[\varphi(\mathbf{0})]d_0(A[\varphi(\mathbf{0})]t; \varphi(\mathbf{0}))$. This is equivalent to a change of the trajectory's period by a factor $A^{-1}[\varphi(\mathbf{0})]$. The statistical effects can be seen in figure 10 where the PDF of the periods $P(T)$ is plotted at different β values with $\alpha = 0$.

https://doi.org/10.1017/S0022377822000022 Published online by Cambridge University Press

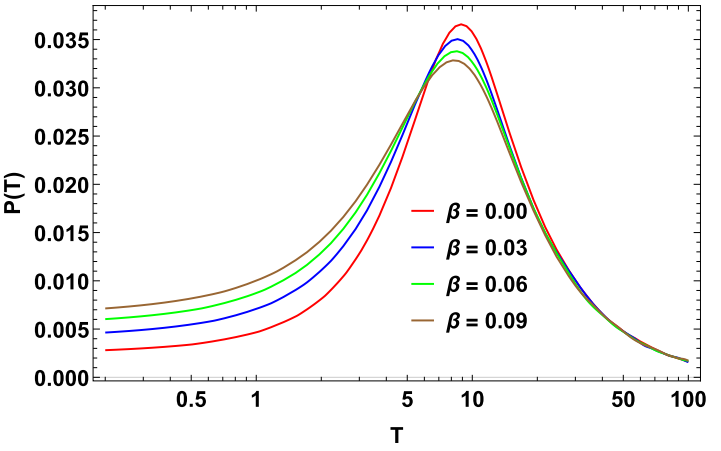

FIGURE 10. PDF $P(T)$ of the trajectory periods at different β values in frozen turbulence $\tau_c \to \infty$ and no poloidal velocity $V_p = 0$.

One can notice that the intermittency lowers the general values of the periods. This is a natural consequence of the fact that $A[\varphi(0)] > 1$. The effect is more pronounced at small and intermediate values $T \sim \tau_{\rm fl}$ since the low-frequency trajectories, i.e. $T \gg \tau_{\rm fl}$, are those with low values of the potential $\varphi(\mathbf{0}) \sim 0$. For the latter, the factor $A[\varphi(\mathbf{0})] \sim 1$.

Although at small times $t \ll \tau_{\rm fl}$ all trajectories contribute to the diffusion, their average is only slightly dependent on β. The effect becomes more pronounced at times of the order of the time of flight. The fact that the distributions of slow trajectories $T \gg \tau_{\rm fl}$ are almost unchanged explains why the asymptotic behaviour of diffusion in the nonlinear regime $K_\star \gg 1$ is universal: the scaling law $D \sim K^{1-\gamma}$ is invariant to non-Gaussianity at $K_\star \gg 1$.

On the other hand, the distribution of potentials is changed. Thus, the effect of non-Gaussianity on diffusion results both from a change in the weight of each equipotential line and from the distortion of time periods.

Furthermore, we underline that, if the turbulence is frozen, both the distribution of Lagrangian potentials and that of Lagrangian velocities (Lumley's theorem, due to the divergenceless property of the Eulerian velocity field) are invariant in time. Under these two strong constrains, it is clear that the only microscopic effect of non-Gaussianity is the redistribution of trajectory frequencies. Other dynamical phenomena which might affect the transport are not present.

Finally, we note how the distribution of small-valued potentials $\phi \ll \Phi$ is virtually unchanged due to the shape of f (the nonlinear mapping between φ and ϕ). These small values are linked to long low-frequency trajectories, thus, to the behaviour of diffusion in the nonlinear regime $K_\star \gg 1$, $\tau_c \gg \tau_{\rm fl}$. This explains why the scaling behaviour (γ) is unchanged by intermittency.

4. Conclusions

In the present work we have analysed the effects of non-Gaussian turbulent electric fields on the turbulent transport in magnetized fusion plasmas. The non-Gaussianity of $\phi(\boldsymbol{x}, t)$ is considered a sign of intermittency and it is designed to be in agreement with experimental data on field statistics. We consider the simple case of $\boldsymbol{E} \times \boldsymbol{B}$ drift-type dynamics in a constant magnetic field in a slab geometry. The transport is characterized by the resulting diffusion coefficient.

https://doi.org/10.1017/S0022377822000022 Published online by Cambridge University Press

In order to mimic the experimental data, the non-Gaussian field ϕ is modelled using a nonlinear transformation f from a fictitious Gaussian turbulent field φ. The transport and the turbulence model are analysed on three distinct levels: analytical, numerical and physical.

The analytical analysis suggests that, for small values of skewness and kurtosis, the diffusion decreases linearly with the excess kurtosis $\delta\kappa$ while the dependency on skewness can be neglected. The numerical analysis, which is performed using two distinct statistical methods (DTM and DNS), confirms the analytical estimations: indeed, only the kurtosis of the non-Gaussian field affects the diffusion in a linear manner. Moreover, exploring numerically the main dependence of the response coefficient $\chi(K_\star)$ on correlation time, an interesting behaviour was found. In the quasilinear regime, the effects of intermittency are small $\chi \to 0$. At the other end of the spectrum, $K_\star \gg 1$, χ saturates to a maximum, which is reached after the time of flight τ_{fl}, i.e. $K_\star = 1 - 2$. The presence of a poloidal velocity induces an algebraic decay of the susceptibility $\chi \sim K_\star^{-\zeta} \to 0$ in the nonlinear regime. To summarize our findings:

$$\begin{cases} D^\infty(\delta\kappa, s) \approx D^\infty(0,0)\,(1 + \chi(K_\star)\delta\kappa) & \\ \chi(K_\star) \propto K_\star^2, & K_\star \ll \tau_{\text{fl}} \\ \chi(K_\star) \sim K_\star^{-\zeta}, & K_\star \gg \tau_{\text{fl}} \\ \max[\chi(K_\star)] \approx \chi(\tau_{\text{fl}} = \tau_c) & \end{cases} \tag{4.1}$$

Our results suggest that the specific correlation time of turbulence τ_c as well as the departure from Gaussianity might serve as control parameters for the anomalous transport of plasma.

Declaration of interests

The authors report no conflict of interest.

Acknowledgements

This work has been carried out within the framework of the EUROfusion Consortium and has received funding from the Euratom research and training programme 2014–2018 and 2019–2020 under grant agreement No. 633053. The views and opinions expressed herein do not necessarily reflect those of the European Commission.

Editor Per Helander thanks the referees for their advice in evaluating this article.

REFERENCES

ANDERSON, J. & BOTHA, G.J.J. 2015 Statistical properties of Charney-Hasegawa-Mima zonal flows. *Phys. Plasmas* **22** (5), 052305, https://aip.scitation.org/doi/pdf/10.1063/1.4919852.

ANDERSON, J. & HNAT, B. 2017 Statistical analysis of Hasegawa-Wakatani turbulence. *Phys. Plasmas* **24** (6), 062301.

ANGIONI, C., FABLE, E., GREENWALD, M., MASLOV, M., PEETERS, A.G., TAKENAGA, H. & WEISEN, H. 2009 Particle transport in tokamak plasmas, theory and experiment. *Plasma Phys. Control. Fusion* **51** (12), 124017.

ANTAR, G.Y., DEVYNCK, P., GARBET, X. & LUCKHARDT, S.C. 2001*a* Turbulence intermittency and burst properties in tokamak scrape-off layer. *Phys. Plasmas* **8** (5), 1612–1624.

ANTAR, G.Y., KRASHENINNIKOV, S.I., DEVYNCK, P., DOERNER, R.P., HOLLMANN, E.M., BOEDO, J.A., LUCKHARDT, S.C. & CONN, R.W. 2001*b* Experimental evidence of intermittent convection in the edge of magnetic confinement devices. *Phys. Rev. Lett.* **87**, 065001.

https://doi.org/10.1017/S0022377822000022 Published online by Cambridge University Press

BEADLE, C.F. & RICCI, P. 2020 Understanding the turbulent mechanisms setting the density decay length in the tokamak scrape-off layer. *J. Plasma Phys*. **86** (1), 175860101.

BOLDYREV, S. 2005 On the spectrum of magnetohydrodynamic turbulence. *Astrophys. J*. **626** (1), L37–L40.

BOURDELLE, C., GARBET, X., IMBEAUX, F., CASATI, A., DUBUIT, N., GUIRLET, R. & PARISOT, T. 2007 A new gyrokinetic quasilinear transport model applied to particle transport in tokamak plasmas. *Phys. Plasmas* **14** (11), 112501.

CASATI, A., GERBAUD, T., HENNEQUIN, P., BOURDELLE, C., CANDY, J., CLAIRET, F., GARBET, X., GRANDGIRARD, V., GÜRCAN, O.D., HEURAUX, S., *et al.* 2009 Turbulence in the tore supra tokamak: measurements and validation of nonlinear simulations. *Phys. Rev. Lett*. **102**, 165005.

CHENG, J., YAN, L.W., HONG, W.Y., ZHAO, K.J., LAN, T., QIAN, J., LIU, A.D., ZHAO, H.L., LIU, Y., YANG, Q.W., *et al.* 2010 Statistical characterization of blob turbulence across the separatrix in HL-2a tokamak. *Plasma Phys. Control. Fusion* **52** (5), 055003.

CLAESSENS, M. 2020 *ITER: The Giant Fusion Reactor*. Copernicus.

CORRSIN, S. 1951 On the spectrum of isotropic temperature fluctuations in an isotropic turbulence. *J. Appl. Phys*. **22** (4), 469–473.

CROITORU, A., PALADE, D., VLAD, M. & SPINEANU, F. 2017 Turbulent transport of alpha particles in tokamak plasmas. *Nucl. Fusion* **57** (3), 036019.

FILIPPAS, A.V., BENGSTON, R.D., LI, G., MEIER, M., RITZ, C.P. & POWERS, E.J. 1995 Conditional analysis of floating potential fluctuations at the edge of the texas experimental tokamak upgrade (text-u). *Phys. Plasmas* **2** (3), 839–845.

FONCK, R.J., COSBY, G., DURST, R.D., PAUL, S.F., BRETZ, N., SCOTT, S., SYNAKOWSKI, E. & TAYLOR, G. 1993 Long-wavelength density turbulence in the TFTR tokamak. *Phys. Rev. Lett*. **70**, 3736–3739.

FÜLÖP, T. & NORDMAN, H. 2009 Turbulent and neoclassical impurity transport in tokamak plasmas. *Phys. Plasmas* **16** (3), 032306.

GAO, X., ZHANG, T., HAN, X., ZHANG, S., KONG, D., QU, H., WANG, Y., WEN, F., LIU, Z. & Huang, C. 2015 Experimental study of pedestal turbulence on EAST tokamak. *Nucl. Fusion* **55** (8), 083015.

GHILEA, M.C., RUFFOLO, D., CHUYCHAI, P., SONSRETTEE, W., SERIPIENLERT, A. & MATTHAEUS, W.H. 2011 Magnetic field line random walk for disturbed flux surfaces: trapping effects and multiple routes to Bohm diffusion. *Astrophys. J*. **741** (1), 16.

GONÇALVES, B., HENRIQUES, I., HIDALGO, C., SILVA, C., FIGUEIREDO, H., NAULIN, V., NIELSEN, A. & MENDONÇA, J. 2018 Radial structure of vorticity in the plasma boundary of tokamak plasmas. In *45th EPS Conference on Plasma Physics*, pp. P2–1084. European Physical Society.

HAUFF, T. & JENKO, F. 2006 Turbulent e × b advection of charged test particles with large gyroradii. *Phys. Plasmas* **13** (10), 102309.

HOLLAND, C., WHITE, A.E., MCKEE, G.R., SHAFER, M.W., CANDY, J., WALTZ, R.E., SCHMITZ, L. & TYNAN, G.R. 2009 Implementation and application of two synthetic diagnostics for validating simulations of core tokamak turbulence. *Phys. Plasmas* **16** (5), 052301.

ISICHENKO, M.B. 1992 Percolation, statistical topography, and transport in random media. *Rev. Mod. Phys*. **64**, 961–1043.

JENKO, F. & DORLAND, W. 2001 Nonlinear electromagnetic gyrokinetic simulations of tokamak plasmas. *Plasma Phys. Control. Fusion* **43** (12A), A141–A150.

JENKO, F. & DORLAND, W. 2002 Prediction of significant tokamak turbulence at electron gyroradius scales. *Phys. Rev. Lett*. **89**, 225001.

KRAICHNAN, R.H. 1968 Small-scale structure of a scalar field convected by turbulence. *Phys. Fluids* **11** (5), 945–953, https://aip.scitation.org/doi/pdf/10.1063/1.1692063.

KRAICHNAN, R.H. & MONTGOMERY, D. 1980 Two-dimensional turbulence. *Rep. Prog. Phys*. **43** (5), 547–619.

KRASHENINNIKOV, S. 2001 On scrape off layer plasma transport. *Phys. Lett.* A **283** (5), 368–370.

LEONARD, A.W. 2014 Edge-localized-modes in tokamaks. *Phys. Plasmas* **21** (9), 090501.

LEVINSON, S., BEALL, J., POWERS, E. & BENGTSON, R. 1984 Space/time statistics of the turbulence in a tokamak edge plasma. *Nucl. Fusion* **24** (5), 527–539.

Lipschultz, B., Bonnin, X., Counsell, G., Kallenbach, A., Kukushkin, A., Krieger, K., Leonard, A., Loarte, A., Neu, R., Pitts, R., *et al.* 2007 Plasma–surface interaction, scrape-off layer and divertor physics: implications for ITER. *Nucl. Fusion* **47** (9), 1189.

Liu, Y., Li, J., Sun, S. & Yu, B. 2019 Advances in Gaussian random field generation: a review. *Comput. Geosci*. **23** (5), 1011–1047.

van Milligen, B.P., Sánchez, R., Carreras, B.A., Lynch, V.E., LaBombard, B., Pedrosa, M.A., Hidalgo, C., Gonçalves, B. & Balbín, R. 2005 Additional evidence for the universality of the probability distribution of turbulent fluctuations and fluxes in the scrape-off layer region of fusion plasmas. *Phys. Plasmas* **12** (5), 052507.

Monin, A. & Yaglom, A. 1973 *Statistical Fluid Mechanics: Mechanics of Turbulence*. MIT Press.

Negrea, M. 2019 Diffusion of stochastic magnetic field lines with average poloidal magnetic component. *Plasma Phys. Control. Fusion* **61** (6), 065004.

Negrea, M., Petrisor, I. & Shalchi, A. 2017 Stochastic field-line wandering in magnetic turbulence with shear. II. Decorrelation trajectory method. *Phys. Plasmas* **24** (11), 112303.

Ottaviani, M. 1992 Scaling laws of test particle transport in two-dimensional turbulence. *Europhys. Lett*. **20** (2), 111–116.

Palade, D.I. 2021 Turbulent transport of fast ions in tokamak plasmas in the presence of resonant magnetic perturbations. *Phys. Plasmas* **28** (2), 022508.

Palade, D.I. & Vlad, M. 2021 Fast generation of gaussian random fields for direct numerical simulations of stochastic transport. *Stat. Comput*. **31** (5), 60.

Palade, D.I., Vlad, M. & Spineanu, F. 2021 Turbulent transport of the w ions in tokamak plasmas: properties derived from a test particle approach. *Nucl. Fusion* **61** (11), 116031.

Pereira, F.A.C., Sokolov, I.M., Toufen, D.L., Guimarães-Filho, Z.O., Caldas, I.L. & Gentle, K.W. 2019 Statistical properties of intermittent bursts in the texas helimak. *Phys. Plasmas* **26** (5), 052301.

Pommois, P., Veltri, P. & Zimbardo, G. 2001 Kubo number and magnetic field line diffusion coefficient for anisotropic magnetic turbulence. *Phys. Rev.* E **63**, 066405.

Qi, L., Kwon, J.-M., Hahm, T., Yi, S. & Choi, M. 2019 Characteristics of trapped electron transport, zonal flow staircase, turbulence fluctuation spectra in elongated tokamak plasmas. *Nucl. Fusion* **59** (2), 026013.

Reuss, J.-D. & Misguich, J.H. 1996 Low-frequency percolation scaling for particle diffusion in electrostatic turbulence. *Phys. Rev.* E **54**, 1857–1869.

Reuss, J.-D., Vlad, M. & Misguich, J. 1998 Percolation scaling for transport in turbulent plasmas. *Phys. Lett.* A **241** (1), 94–98.

Riva, F., Militello, F., Elmore, S., Omotani, J.T., Dudson, B., Walkden, N.R. & the MAST team 2019 Three-dimensional plasma edge turbulence simulations of the mega ampere spherical tokamak and comparison with experimental measurements. *Plasma Phys. Control. Fusion* **61** (9), 095013.

Shafer, M.W., Fonck, R.J., McKee, G.R., Holland, C., White, A.E. & Schlossberg, D.J. 2012 2D properties of core turbulence on DIII-D and comparison to gyrokinetic simulations. *Phys. Plasmas* **19** (3), 032504.

Vio, R., Andreani, P. & Wamsteker, W. 2001 Numerical simulation of non-Gaussian random fields with prescribed correlation structure. *Publ. Astron. Soc. Pacific* **113** (786), 1009.

Vlad, M., Palade, D.I. & Spineanu, F. 2021 Effects of the parallel acceleration on heavy impurity transport in turbulent tokamak plasmas. *Plasma Phys. Control. Fusion* **63** (3), 035007.

Vlad, M. & Spineanu, F. 2016 Direct effects of the resonant magnetic perturbation on turbulent transport. *Nucl. Fusion* **56** (9), 092003.

Vlad, M., Spineanu, F., Misguich, J.H. & Balescu, R. 1998*a* Diffusion with intrinsic trapping in two-dimensional incompressible stochastic velocity fields. *Phys. Rev.* E **58**, 7359–7368.

Vlad, M., Spineanu, F., Misguich, J.H. & Balescu, R. 1998*b* Diffusion with intrinsic trapping in two-dimensional incompressible stochastic velocity fields. *Phys. Rev.* E **58**, 7359–7368.

Vlad, M., Spineanu, F., Misguich, J.H. & Balescu, R. 2001 Diffusion in biased turbulence. *Phys. Rev.* E **63**, 066304.

VLAD, M., SPINEANU, F., MISGUICH, J.H., REUSS, J.-D., BALESCU, R., ITOH, K. & ITOH, S.-I. 2004 Lagrangian versus eulerian correlations and transport scaling. *Plasma Phys. Control. Fusion* **46** (7), 1051–1063.

WANG, L., TYNAN, G.R., HONG, R., NIE, L., CHEN, Y., KE, R., WU, T., LONG, T., ZHENG, P. & XU, M. 2019 Edge turbulence evolution and intermittency development near the density limit on the HL-2A tokamak. *Phys. Plasmas* **26** (9), 092303.

WANG, W.X., LIN, Z., TANG, W.M., LEE, W.W., ETHIER, S., LEWANDOWSKI, J.L.V., REWOLDT, G., HAHM, T.S. & MANICKAM, J. 2006 Gyro-kinetic simulation of global turbulent transport properties in tokamak experiments. *Phys. Plasmas* **13** (9), 092505.

ZANK, G.P., DOSCH, A., HUNANA, P., FLORINSKI, V., MATTHAEUS, W.H. & WEBB, G.M. 2011 The transport of low-frequency turbulence in astrophysical flows. I. Governing equations. *Astrophys. J.* **745** (1), 35.

ZOHM, H. 1996 Edge localized modes (ELMs). *Plasma Phys. Control. Fusion* **38** (2), 105–128.

ZWEBEN, S.J., BOEDO, J.A., GRULKE, O., HIDALGO, C., LABOMBARD, B., MAQUEDA, R.J., SCARIN, P. & TERRY, J.L. 2007 Edge turbulence measurements in toroidal fusion devices. *Plasma Phys. Control. Fusion* **49** (7), S1–S23.

https://doi.org/10.1017/S0022377822000022 Published online by Cambridge University Press